In-situ analysis on formation and development of LPSO-like nanostructures in dilute MgYZn and MgGdZn alloys (TMS 2022 proceedings, Magnesium Technology, accepted Oct.2021, issued Feb. 2022)

Hiroshi Okuda[1], Michiaki Yamasaki[2], Yoshihito Kawamura[2]

1. Department of Materials Science and Engineering, Kyoto University, Kyoto 606-8501 Japan,
2. Magnesium Research Center and department of Materials Engineering, Kumamoto University, Kumamoto 860-8555 Japan.

Abstract Precipitation process leading to the formation of long-period stacking ordered (LPSO) structures in dilute MgGdZn and MgYZn alloys during heating at a heating rate of 10 K/min have been examined by in-situ synchrotron radiation small- and wide-angle scattering measurements. Samples were solution-treated and quenched prior to the measurements. During heating, two distinct temperature regions were observed for both alloys. The one at the lower temperature, clusters without in-plane order appeared, and then dissolved at higher temperatures. Clusters leading to LPSO structures appeared at a higher temperature above 600 K. Streaky peaks appeared above the temperature, suggesting that very thin layers of LPSO structure with relatively large domain size in the in-plane direction were formed. The average cluster-cluster distance in the segregation layer above 600 K was almost constant until dissolution of LPSO structure at 800 K. The average cluster –cluster distance is larger than the ideally ordered superstructures reported for stoichiometric LPSO alloys.

Keyword: MgGdZn, MgYZn, dilute LPSO alloy, synchrotron radiation small-angle scattering, in-situ measurements

Hiroshi OKUDA, Department of Materials Science and Engineering, Kyoto University, Sakyo-ku Kyoto 606-8501 Japan.
okuda.hiroshi.5a@kyoto-u.ac.jp

Michiaki YAMASAKI, Magnesium Research Center and Department of Materials Science, Kumamoto University, Kurokami, Kumamoto 860-8555 Japan.
Yamasaki @gpo.kumamoto-u.ac.jp

Yoshihito KAWAMURA, Magnesium Research Center and Department of Materials Science, Kumamoto University, Kurokami, Kumamoto 860-8555 Japan.
rivervil@gpo.kumamoto-u.ac.jp

Introduction

Controlling the formation of partial structures of long-period stacking ordered structure in dilute MgYZn alloys has been expected to be a prospective approach to strengthen Mg based materials without increasing specific weight. To understand the formation kinetics, however, in-situ approach is important, since the phase transformation process in dilute MgYZn alloys is expected to be thermal history dependent, and many intermediate structures may appear. About two decades after the findings of LPSO structures by Kawamura et al. [1]-[4], they reported a possible approach of controlling kink microstructures in dilute MgYZn alloys [5]. Since the process is dependent on the preparation processes including thermal history, we undertook in-situ measurements of dilute MgYZn and MgGdZn alloys. These alloy systems have been well examined also from a phase diagram viewpoint [6]-[8].

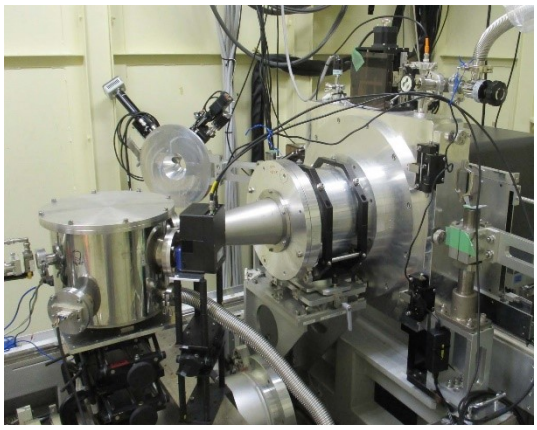

Fig.1 In-situ SWAXS measurement system used in the present work. In-situ chamber with a WAX detector (left), beam path (middle) and Pilatus2M (rightmost).

Experimental

We performed in-situ small- and wide- angle X-ray scattering (SWAXS) measurements to examine nanostructural evolution during heat treatments [9]-[11]. SWAXS measurements have been performed at beam-line 40B2 of SPring8, Hyogo Japan with a photon energy of 12.4 keV. To examine so-called $L1_2$ clusters characteristic for LPSO structures and their precursory clusters, SAXS measurements covered up to q = 8 nm^{-1} by using a Pilatus 2M detector, where q is the modulus of the scattering vector defined by,

$$q = 4\pi \sin(\theta) / \lambda \ .$$

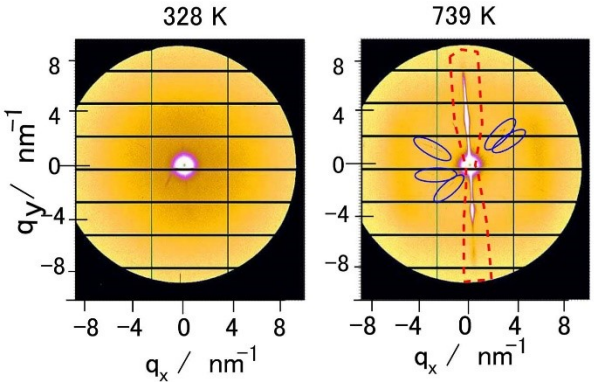

Fig.2 Two-dimensional SAXS profiles at 328 K and 739 K. Black lines are gaps of the detector unit.

$Mg_{98.6}Y_1Zn_{0.4}$ and $Mg_{97}Gd_2Zn_1$ alloys have been solution treated at 802 K and 793 K for 10 min. respectively, where the compositions are given by at%. For MgGdZn alloys, samples were cut from an ingot of a diameter of 28 mm. For MgYZn alloy, the samples were cut from liquid-quenched and hot-pressed sample. They were wrapped by a graphite sheet and sealed in evacuated Pyrex® tubes for solution treatment and quenched into iced water. In-situ measurements were performed by heating the samples at a heating rate of 10 K/min in the in-situ SWAXS apparatus. Figure 1 gives a photograph of the SWAXS system used in the present work. To suppress

oxidation and evaporation, the samples were sealed by graphite films and the in-situ chamber was evacuated by a turbo molecular pump.

Results and Discussions

Figure 2 gives two examples of two-dimensional SAXS intensity profiles during heating a solution treated $Mg_{97}Gd_2Zn_1$ sample. The SAXS intensities taken by a two-dimensional detector suggest that the intensity profile after quench is isotropic and monotonically decreases with the magnitude of the scattering vector, q, as shown for 328 K in the figure. For the profile obtained for 739 K, well-defined streaks appear as surrounded by the broken lines. Short streaks marked by solid ellipses are the ones whose orientation do not agree with the Ewald sphere and they are not used for the analysis. Isotropic component is also observed, whose diffuse peak appears at q~5.2 nm^{-1}.

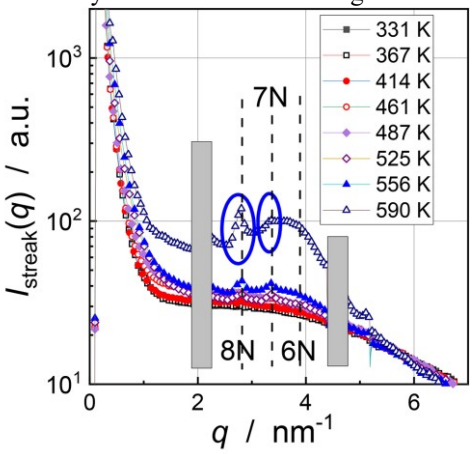

Fig.3 SAXS intensity along the streak at lower temperatures. Periodicity of 24R, 14H, 18R are denoted by 8N, 7N, and 6N since SAXS peaks only reflect periodicity of compositional modulation.

To examine the streak components and the diffuse components, the area on the detector that streaks appear at higher temperatures was registered as fixed ROI (range of interest) throughout the in-situ measurement to evaluate the scattering intensity along the streak. For the diffuse scattering part, all the detector pixels that the streak component never appear throughout the heating process were used to take the radial average as a function of q.

The change of the SAXS intensity along the streak during heating at 10 K/min. is shown for lower temperature in Fig. 3. As shown in Fig.2, the streak components suffer from lack in the data region due to gaps between detector elements, which are masked by two filled rectangles in the figure, while no gap was observed for diffuse scattering calculated by the radial average. The SAXS profile decreased monotonically with q for the as-quenched condition. As the temperature increases, SAXS intensity only slowly increases up to about 560 K. For the corresponding temperatures, small and relatively sharp peaks were found at 2.9 nm^{-1} and 3.4 nm^{-1}, which correspond to reported 24R and 14H periodicity of the LPSO structures [9][12]. Below 560 K, the peaks do not grow much. In contrast to the sharp and small peaks, a broad peak whose width covers

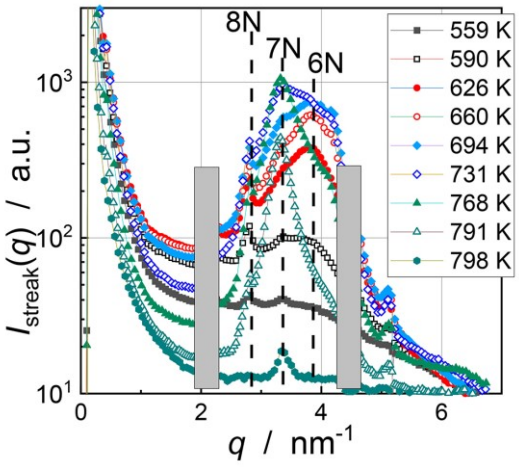

Fig.4 SAXS intensity along the streak for higher temperatures,

the two peak positions and the 6N peak position started to grow much faster than the preceding small and sharp peaks between 556 K and 581 K. The change of the SAXS intensity along the streaks above 581 K is shown in Fig. 4. The peak position of the broad peaks in Fig.4 do not agree with the exact position of the LPSO periodicity in the early stage, i.e., below 750 K, while the peak position converged to about 3.4 nm-1 which agrees with the reported stable periodicity of 14H reported for MgGdZn alloys[10][13]. Broad peak in Fig.4 is explained by a finite thickness of segregation layers, since the compositions of the present samples are far less than the stoichiometry of the LPSO structures [6] [12] and a solution treatment may lead to nucleation of segregation / stacking fault layers randomly and separately in space[5]. Assuming that the periodical segregation gives a diffraction peak, a simple estimation of thickness from the diffraction gives

$$t \sim 2\pi/\Delta q \qquad (1)$$

where t is the thickness of the domain, Δq is the FWHM of the peak. The estimated thickness was 3.4 nm at 598 K, 5.1 nm at 633.8 K, and 6.0 nm at 660 K where the peak remained single peak at 6N position up to 680 K. After the average periodicity shifts to that of 14H, the peak sharpened to a value corresponding to t~18 nm at 790.1 K.

The isotropic component of the same measurements shown in Fig.4 is given in Fig.5. The isotropic SAXS profile start showing a well-defined peak around q~5.2 nm^{-1} above 700 K. The well-defined peak is characteristic for in-plane interference of $L1_2$ clusters [9]-[11]. The peak position increased slightly from 4.8 nm^{-1} at 610 K to 5.1 nm^{-1} at 675 K, until complete dissolution of the LPSO structure, i.e., solution treated state. The in-plane distance of $L1_2$ clusters in the stacking fault layer calculated from the peak position of Fig.5 is much larger than the reported ideal $2\sqrt{3}$ x $2\sqrt{3}$ prototype superstructures [14]-[17], whose peak position should appear at q ~ 6.2 nm^{-1}. For the in-plane distance of LPSO structure of cast $Mg_{97}Y_2Zn_1$ alloy, ex-situ measurements of long-time isothermal annealing revealed that the two-dimensional arrangement of $L1_2$ clusters on the segregation layer is far disordered, and the average distance between the nearest clusters is much larger even after long-time annealing. For example, the in-plane peak position of $Mg_{97}Y_2Zn_1$ ingot after annealing at 673 K for 1 month is still 5.3 nm^{-1}[9]. Therefore, the transformation process in solution-treated $Mg_{97}Gd_2Zn_1$ alloys during heating can be divided into two regions, i.e., (A) low temperature region below 600 K, where no planar segregation layer was observed and scattering by cluster is rather monotonic, and (B) higher temperature region above 600 K where well-

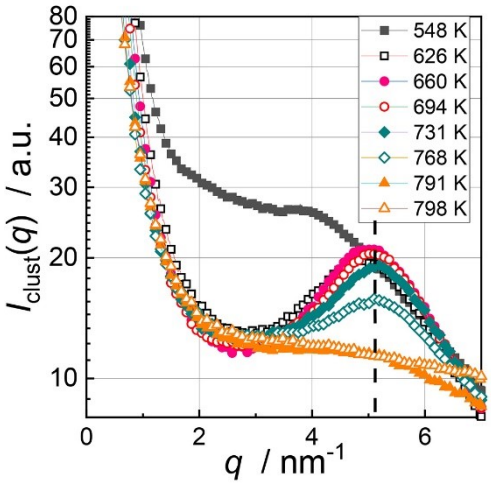

Fig.5 SAXS intensity of isotropic component for T>580 K, showing in-plane array of clusters.

defined streaks with characteristic in-plane cluster-cluster correlation peak appear. The nanostructure appearing in the region B corresponds to LPSO structures with small thickness and /or mixture of stacking interval of mainly 6 and 7 atomic layers in c axis of the hcp matrix.

Figure 6 shows the radially averaged SAXS intensity of $Mg_{98.6}Y_1Zn_{0.4}$ alloy during heating. The radial average was taken for all the area without separating streak and isotropic components, because sharp streaks appear very densely, and hard to separate them from the isotropic area. This is due to the sample preparation process that the MgYZn sample was prepared by hot pressing, resulting in randomly oriented small grains of less than 40 micrometer in diameter, in comparison with several handred micrometers for the cast MgGdZn samples. The intensity map also shows two regions, the low temperature region below 600 K and above 600 K whose peak temperatures are shown by the horizontal arrows. Similar to the GdZn case, the SAXS intensity at low temperature region is monotonically decreasing with q. For higher temperature region, very narrow and weak but densely dispersed streaks were observed, which lead to a weak and broad peak whose peak position is not as well-defined as those for GdZn case, but observed around the peak position corresponding to 14H as shown by the vertical arrow in the figure. In-plane cluster interference was also observed only for the upper temperature region, meaning that in-plane $L1_2$ cluster arrangement was expected above 600K.

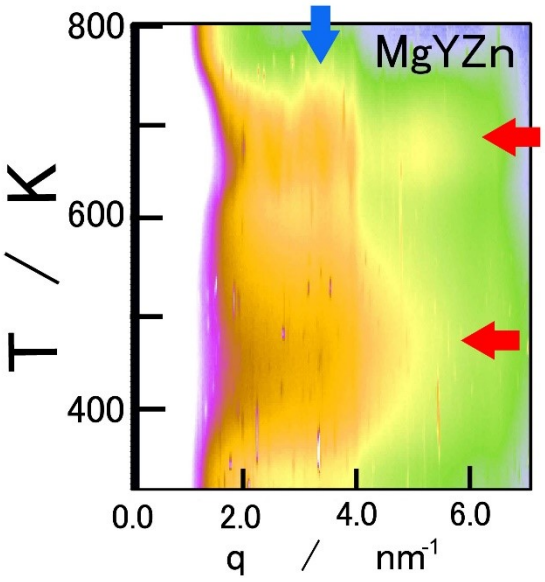

Fig.6 Radially averaged SAXS intensity of the MgYZn sample.

Compared with the results for GdZn sample, the in-plane interference peak is weaker in the YZn sample, still, as shown by the upper horizontal arrow, interference peak ssimular to the one for GdZn sample was observed. Therefore, the transition from non-LPSO type clusters at low temperatures to thin LPSO structure at higher temperature at around 600 K occurs in common. The temperature is about 50 K higher than the one observed for the introduction of stacking faults in $Mg_{85}Y_9Zn_6$ supersaturated alloys[17] whose kinetics was explained by activation energy of the introduction of stacking faults.

Conclusion

In summary, in-situ synchrotron radiation SWAXS measurements have been made for dilute MgGdZn and MgYZn alloys after solution treatments. The SAXS profile during heating at 10 K/min reveals two-step transformation sequence of clustering without plate-like microstructure at lower temperatures and then the plate-like microstructures with $L1_2$ clusters, i.e., a thin precursory LPSO structures at higher

temperatures. Reported heat treatment temperature that contribute to strengthening belong to the lower temperature side of the higher temperature region.

Present work has been financially supported by grant-in-aid for scientific research from JSPS, grant number 18H05476 and Light Metals Education Foundation. SWAXS measurements have been made under approval of 2016B1279, 2021A1241 at SPring8 and 2017G593 and 2019G685 at Photon Factory, Japan.

References

[1] Kawamura Y, Hayashi K, Inoue A, Masumoto T (2001) Rapidly Solidified Powder Metallurgy $Mg_{97}Zn_1Y_2$ Alloys with Excellent Tensile Yield Strength above 600 MPa, Mater. Trans. **42**:1172–1176.

[2] Kawamura Y, Yamasaki M (2007) Formation and mechanical properties of Mg97Zn1Y2 alloys with long-period stacking ordered structure, Mater. Trans. **48:** 2986-2992.

[3] Hagihara K, Yokotani N, Umakoshi Y, (2010) Plastic deformation behavior of Mg12YZn with 18R long-period stacking ordered structure, Intermetallics **18:**267–276

[4] Yamasaki M, Sasaki M, Nishijima M, Hiraga K, Kawamura Y(2007) Formation of 14H long period stacking ordered structure and profuse stacking faults in Mg-Zn-Gd alloys during isothermal aging at high temperature, Acta Mater. **55:** 6798–6805.

[5] Hagihara K, Ueyama R, Yamasakki M, Kawamura Y(2021) Surprising increase in yield stress of Mg single crystal using long-period stacking ordered nanoplates, Acta Mater. **209:**116797.

[6] Gröbner J, Kozlov A, Feng XY, Geng J, Nie JF, Schmid-Fetzer R (2012) Phase equilibria and transformation in ternary Mg-rich Mg-Y-Zn alloys, Acta Mater. **60:**5948–5962.

[7] Gröbner J, Kozlov A, Fang X-Y, Zhu S, Nie JF, Gibson M, Schmid-Fetzer R(2015) Phase Equilibria and transformations in ternary Mg-GdZn alloys. Acta Materialia **90:**400-416.

[8] Minamoto S, Nomoto S, Hamaya A, Horiuchi T, Miura S (2010)Microstructure Simulation for Solidification of Magnesium-Zinc-Yttrium Alloy by Multi-phase-field Method Coupled with CALPHAD Database, ISIJ international **50**:1914-1919.

[9] Okuda H, Horiuchi T, Hifumi S, Yamasaki M, Kawamura Y, Kimura S(2014) Microstructural evolution of Long-period stacking ordered structures in $Mg_{97}Y_2Zn_1$ alloys examined by in-situ small-angle x-ray scattering, Metall. Trans. **45**A: 4780-4785.

[10] Okuda H, Horiuchi T, Tanaka H, Yamasaki M, Kawamura Y, Kimura S (2015)Stability of Long-period stacking ordered structures at elevated temperatures examined by multicolor synchrotron radiation X-ray scattering/diffraction measurements, Materials Transactions **56:**906-909.

[11] Okuda H, Horiuchi T, Maruyama T, Yamasaki M, Kawamura Y, Hagihara K, Kohara S(2014) Development of microstructures of Long-period stacking ordered structures in Mg85Y9Zn6 alloys annealed at 673 K (400C) examined by small-angle X-ray Scattering, Metall. Trans. **45**A:147-151.

[12]Abe E, Ono A, Itoi T, Yamasaki M, Kawamura Y (2011)Polytypes of long-period stacking structures

synchronized with chemical order in dilute MgZnY alloy, Phil. Mag. Letters, **91:**690-696.
[13] Okuda H, Yamasaki M, Kawamura Y(2017) Transition to long period stacking ordered structures in $Mg_{85}Gd_9Zn_6$ alloys from amorphous ribbons examined by synchrotron radiation scattering: comparison with Mg85Y9Zn6 alloys, Scripta Mater. **139:**26-29.
[14] Yokobayashi H, Kishida K, Inui H, Yamasaki, M, Kawamura Y (2011) Enrichment of Gd and Al in the quadruple close packed planes and their in-plane long-range ordering in the long period stacking-ordered phase in the Mg-Al-Gd system, Acta Mater. **59:**7287–7299.
[15] Saal JE, Wolverton C (2014) Thermodynamic stability of Mg-based ternary long-period stacking ordered structures, Acta Mater. **68** :325–338.
[16] Kishida K, Nagai K, Matsumoto A, Yasuhara A, Inui H (2015) Crystal structures of highly ordered long-period stacking –ordered phases with 18R, 14H and 10H-type stacking sequences in the Mg-Zn-Y system, Acta Mater. **99:**228–239.
[17] Okuda H, Yamasaki M, Kawamura Y (2020)Structural and diffusional phase transformations in liquid-quenched $Mg_{85}Y_9Zn_6$ ribbons below the bifurcation temperature, Acta Mater.**194:** 587-593.